Journal of Physics D: Applied Physics

Schottky effect on the wavelength threshold for the photo-detachment from charged metallic nanoparticles

To cite this article before publication: Mikhail Shneider *et al* 2023 *J. Phys. D: Appl. Phys.* in press https://doi.org/10.1088/1361-6463/acce49

Schottky effect on the wavelength threshold for the photo-detachment from charged metallic nanoparticles

Mikhail N. Shneider[1,*], Yevgeny Raitses[2] and Shurik Yatom[2]

[1]*Department of Mechanical and Aerospace Engineering, Princeton University, Princeton, New Jersey 08544, USA*

[2]*Princeton Plasma Physics Laboratory, Princeton, New Jersey 08540, USA*

[*]m.n.shneider@gmail.com

Abstract

Laser-stimulated electron photo-detachment (LSPD) from nanoscale dust particles is predicted to strongly depend on the particle size. A theory of the electron photo-detachment from charged spherical metallic nanoparticles is presented. This theory is relevant to laser-stimulated photo-detachment applied to measurements of charge of nanoparticles in plasmas. Our theory predicts that the charging of nanoparticles in plasma leads to the appearance of an additional electric field, causing a change in the potential barrier at the particle boundary and consequently, a change in the effective work function, due to the Schottky effect. In this case, the critical wavelength of the laser depends not only on the work function, but also on the charge of the nanoparticles and their size.

Dusty plasmas can be found in astrophysical environments (the interstellar medium, cometary tails and planetary ring systems [1,2]), laboratory plasma experiments [3,4], magnetic fusion devices [5], and industrial applications such as semiconductor material processing [6,7] and synthesis of nanomaterials in plasmas [8,9]. In all these environments, the interactions of dust particles with the plasma result in formation of a sheath, which governs their charging. These interactions involve fluxes of electrons and ions from the plasma to the particles and may also be accompanied by electron emission from these particulates back to the plasma. The latter can be driven by thermionic emission and/or field emission as well as photoemission mechanisms, which depend on particle characteristics such as surface temperature and material properties. This charging affects the transport and dynamic behavior of dust particles in the plasma, including their self-organization into coherent structures. Particle charging can also affect the growth of nanoparticles. A complete understanding of such processes requires knowledge of both the spatial and temporal variations of particle charging in the plasma. In this regard, the measurement of the charge of dust particles is a challenging problem. In this paper, we focus on laser-stimulated photo-detachment (LSPD) of electrons from dust particles which was already demonstrated as a promising method for the determination of the particle charge in plasma in real time and in situ [10, 11]. There are certain aspects of this method for dust particles which still need to be addressed, for example the dependence of electron photo-detachment on particle size.

Laser radiation with photon energies exceeding the binding energy of electrons captured by particles (typical values of the affinity energy, ~ 2-4 eV [12]) will cause photo-detachment of electrons (Fig. 1). This process is generally like the photo-detachment of electrons from negative ions, which was extensively studied both theoretically and experimentally, in the presence and absence of plasma [13,14,15]. This LSPD process in plasma is determined by two key parameters: the binding energy of photoelectrons and the photo-detachment cross section. In addition, for dielectric dust particles the photo-detachment may also be affected by the sticking coefficients of electrons arriving from the plasma to the particle surface. These ideas were already expressed in the literature [10,16-19].

In this Letter, we theoretically explore the dependence of the electron photo-detachment threshold on the charge and the size of the dust particle. The charging of nanoparticles leads to the appearance of an additional electric field, leading to a change in the potential barrier at the particle boundary and consequently, a change in the effective work function due to the Schottky effect [20]. In this case, the critical wavelength of the laser (minimum energy required for detachment which is the red border of the photoelectric effect) depends on the charge of the nanoparticles and their size. Finally, we propose an experiment to validate these predictions.

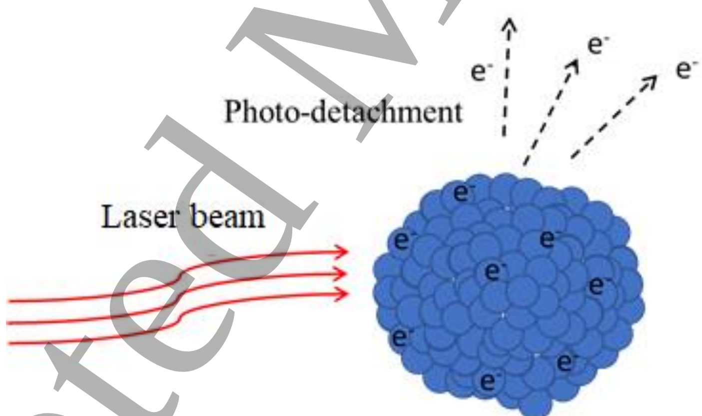

FIG. 1. Schematic of electron LSPD from dust particles in plasma [21]. A recharging of nanoparticles by plasma electrons is not shown.

Particles in a non-equilibrium weakly ionized plasma are charged to a local floating potential, φ_s, when the total current of electrons and ions per particle vanishes [22,23]. In the absence of the electron emission from the particle, its floating potential is given by

$$|\varphi_s| = \frac{kT_e}{e} ln\left[\left(\frac{MT_e}{mT_i}\right)^{1/2} / \left(1 + \frac{e|\varphi_s|}{kT_i}\right)\right], \qquad (1)$$

where T_e, T_i are electron and ion temperatures in plasma; m, M are electron and ion masses, respectively. For dusty plasma cases considered here, particles are charged negative, i.e., electrons are sitting on the particle surface. We shall call these electrons on the surface acquired by particles in the plasma excess electrons. For spherical particles of radius R, the charge obtained in the plasma Q can be deduced from the particle capacitance:

$$Q = 4\pi\varepsilon_0 R\varphi_s. \tag{2}$$

For an excess electron to detach from the particle, it should overcome a potential barrier which is formed in the vicinity of the conductive (metal) particle boundary (Fig. 2) and changes with the distance from the particle, r. This potential barrier is determined by the interaction potential of this emitted electron with the sum of the image force fields [24],

$$\varphi_{im} = -\frac{e^2R^3}{4\pi\varepsilon_0 r^2(r^2-R^2)}, \quad r > R, \tag{3}$$

and the electric field induced by the surface charge,

$$E_Q = \begin{cases} \frac{1}{4\pi\varepsilon_0}\frac{Q}{r^2}, & r \geq R \\ 0, & r < R \end{cases}. \tag{4}$$

For typical parameters of non-equilibrium dusty plasmas, the microscopic field in plasma $E_{pl} \sim T_e/\Lambda_D$ can be neglected compared to E_Q, where $\Lambda_D = \left(\frac{\varepsilon_0 k_B T_e}{n_e e^2}\right)^{1/2}$ is the Debye screening length in plasma. Then, the potential barrier in the vicinity of the charged metal particle can be expressed as

$$\Delta W(R,Q,r) = \varphi_{im} - \varphi_{sf},$$

and can be rewritten as

$$\Delta W(R,Q,r) = -\frac{e^2R^3}{4\pi\varepsilon_0 r^2(r^2-R^2)} - \frac{e}{4\pi\varepsilon_0}\int_R^r \frac{Q}{r^2}dr = -\frac{e^2R^3}{4\pi\varepsilon_0 r^2(r^2-R^2)} + \frac{eQ}{4\pi\varepsilon_0}\left(\frac{1}{r} - \frac{1}{R}\right). \tag{5}$$

Here, φ_{sf} is the contribution to the potential barrier from the surface potential. The extremum condition for the potential barrier is when it does not change with the distance from the particle (Fig. 2),

$$\frac{\partial \Delta W(R,Q,r)}{\partial r} = 0. \tag{6}$$

Using Eqs. (2) and (5), it follows from Eq. (6) that

$$\frac{eR^3(2r^2-R^2)}{r(r^2-R^2)^2} = 4\pi\varepsilon_0 R|\varphi_s|, \tag{7}$$

where φ_s is defined by Eq. (1). Hence, it is possible to determine the position of the extremum, $r = r_m$, where r_m is the solution of the equation (7). At this extremum, the potential barrier (Eq. (5)) acts as the Schottky barrier reduction $\Delta W_{Sch}(R, Q)$ in the vicinity of a charged spherical metal particle:

$$\Delta W_{Sch}(R, Q) = \Delta W(R, Q, r_m). \qquad (8)$$

Let us assume, for definiteness, that spherical nanoparticles are in a nonequilibrium weakly ionized nitrogen plasma with ion temperature T_i=300 K. Calculations were carried out for two cases of electron temperature T_e=1 and 2 eV. The corresponding floating potentials are $\varphi_s = -2.62$ and -4.75 V. Figure 3 shows the calculated positions of the potential barrier extremum $\Delta r = r_m - R$ (Fig. 3a) and the corresponding values of the decreasing potential barrier due to the Schottky effect, $\Delta W_{Sch}(R, Q)$ (Fig. 3b).

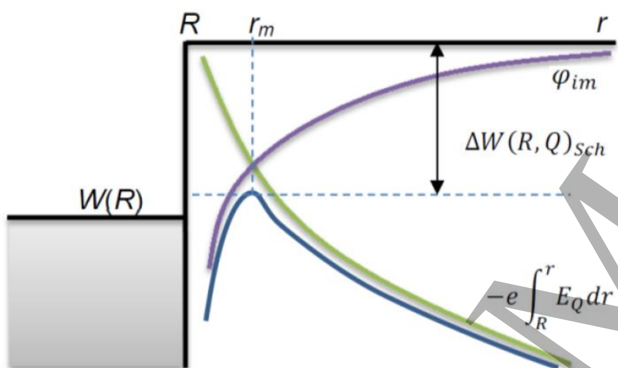

FIG. 2. Scheme of Schottky barrier reduction for a charged spherical metal particle.

The potential barrier reduction described above decreases the energy threshold required for the electron photo-detachment. This effect can be important for the application of the photo-detachment technique to charge measurements of dust particles in dusty plasmas, especially for nanoparticles. Let us consider an experiment in which a tunable laser is used to irradiate nanoparticles immersed into a plasma. The laser wavelength is scanned from long to short wavelengths. The electrons will be detached from the dust particles only when the wavelength matches or exceeds the energy of the potential barrier. For a negatively charged particle, the potential barrier reduction is expected to change the wavelength of the tunable laser at which the electron photo-detachment occurs (so-called red border).

The energy threshold at the red border of the photoemission depends on the type of emitted electrons: excess electrons acquired by the surface exposed to the plasma or "bulk" electrons from the particle material. In the former case, the process of photoemission (aka photoelectric effect) is by photo-detachment which has the threshold defined as the "affinity". In the latter case, the process of photoemission is "ionization" (see, for example Ref. [25]). The difference between the photo-detachment and the photoemission is determined by their corresponding values of the potential (energy) barrier, $W(R)$ [25], which can also be affected by the particle size (Fig. 3).

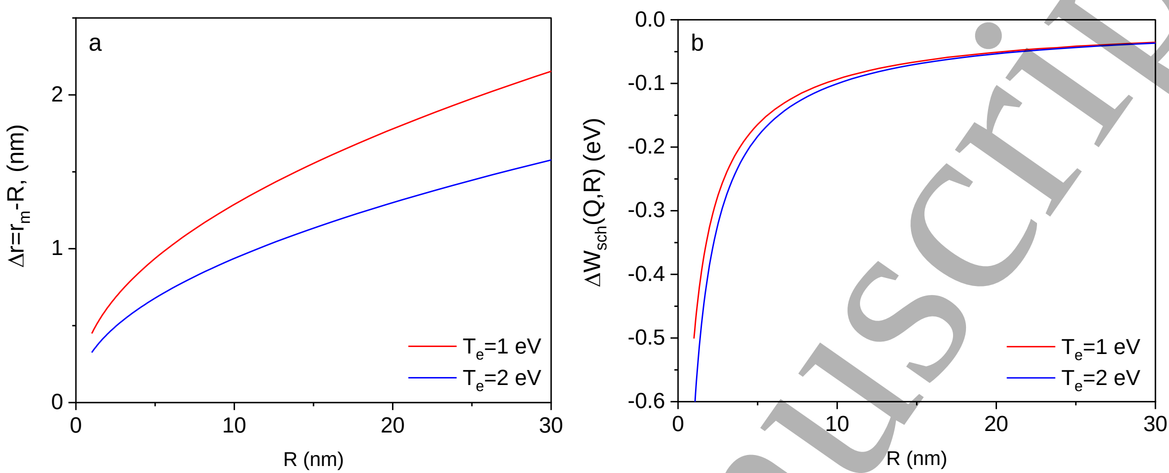

FIG. 3**.** (a) The position of the potential barrier extremum in the vicinity of the particle boundary determined by solving equation (7); (b) - the corresponding values of the barrier decrease (8), due to the Schottky effect. Calculations were carried out for a nonequilibrium nitrogen plasma with T_i=300 K and for two cases of electron temperature T_e=1 and 2 eV. The corresponding floating potentials are $\varphi_s = -2.62$ and -4.75 V.

For a spherical metal particle, $W(R)$ is the effective work function. The value of the $W(R)$ for the electronic affinity is given by [25]:

$$W_A(R) = W_\infty - \frac{5}{8}\frac{e^2}{4\pi\varepsilon_0 R}, \qquad (10)$$

whereas, for the emission of the bulk electrons [25-27]:

$$W_I(R) = W_\infty + \frac{3}{8}\frac{e^2}{4\pi\varepsilon_0 R}. \qquad (11)$$

Here, W_∞ is the work function of the bulk material. With increasing particle radius > 10 nm, $W_A(R) \approx W_I(R) \approx W_\infty$. For smaller nanoparticles with sizes $R < 10$ nm, the difference between $W_A(R)$ and $W_I(R)$ becomes significant [25]. Hence, the corresponding red borders for photo-detachment are as follow: for the laser frequency,

$$\omega_{A,I,cr} = W_{A,I}(R)/\hbar, \qquad (12)$$

where $\hbar$ is the reduced Plank constant, and for the laser wavelength,

$$\lambda_{A,I,cr} = 2\pi c/\omega_{A,I,cr}. \qquad (13)$$

Indices A and I in Eqs. (12) and (13) and below correspond to the cases of photo-detachment of attached electrons and photoemission of bulk electrons corresponding to effective work functions described by Eqs. (10) and (11).

It is important to note that for the detachment of excess electrons acquired by particles in plasma and for the emission of bulk electrons from the particle, the Schottky barrier reduction $\Delta W(R,Q)_{Sch}$, the position of the maximum r_m and the corresponding frequency shifts of the red borders (Eq. (12)) are the same and defined as

$$\Delta\omega = \Delta W(R,Q)_{Sch}/\hbar. \tag{14}$$

However, the shifts of the wavelengths corresponding to the red boundaries of electron affinity and "ionization" (i.e. the effective work function) will be different and can be expressed as

$$\Delta\lambda_{A,I}(R,Q) = -\frac{\Delta\omega\lambda_{A,I,cr}^2}{2\pi c}. \tag{15}$$

From Eqs. (10)-(13) it follows that for laser radiation irradiating negatively charged metal nanoparticles, $\lambda_A \geq \lambda_I$ is satisfied and therefore, the wavelength

$$\widetilde{\lambda_A} = \lambda_A + \Delta\lambda_A(R,Q) \tag{16}$$

corresponds to the red border of the electron photo-detachment of spherical charged nanoparticles. Here, λ_A is the wavelength corresponding to the red border for the photo-detachment in the case of a flat uncharged surface. $\Delta\lambda_A(R,Q)$ is the wavelength shift defined by Eq. (15), which depends on the particle size and charge and is determined by Schottky effect.

To illustrate the effect of particle size on the red borders, we consider silver and lithium nanoparticles with the work functions correspond to the case of uncharged flat surface, $W_\infty =$ 4.5 and 2.9 eV, respectively [28]. The corresponding red borders for electron affinity and "ionization" for these nanoparticles of different radii, without considering the Schottky effect, are shown in Fig. 4. In addition, Fig. 5 shows variations in the critical laser wavelength at which electron photo-detachment occurs when metal nanoparticles of different sizes are irradiated.

From the above analysis, it follows that measurement of the wavelength at which electron photoemission from uncharged particles of known material occurs should allow one to determine the size of the particles. Moreover, measurement of the shift of the red border for photo-detachment for charged particles allows one to find the charge Q acquired by the particles in plasma. The measured value of $\Delta\lambda(R,Q)$ is uniquely determined by the radius of the particles and their charge. Thus, the LSPD diagnostic should allow measurements of both size and charge of particles in dusty plasma. However, given that the dependence of the red border shift on the radius of nanoparticles is much stronger than the dependence on their charge, in practice it is better to use the method considered in this work to determine the charge of nanoparticles for nanoparticles of a known size.

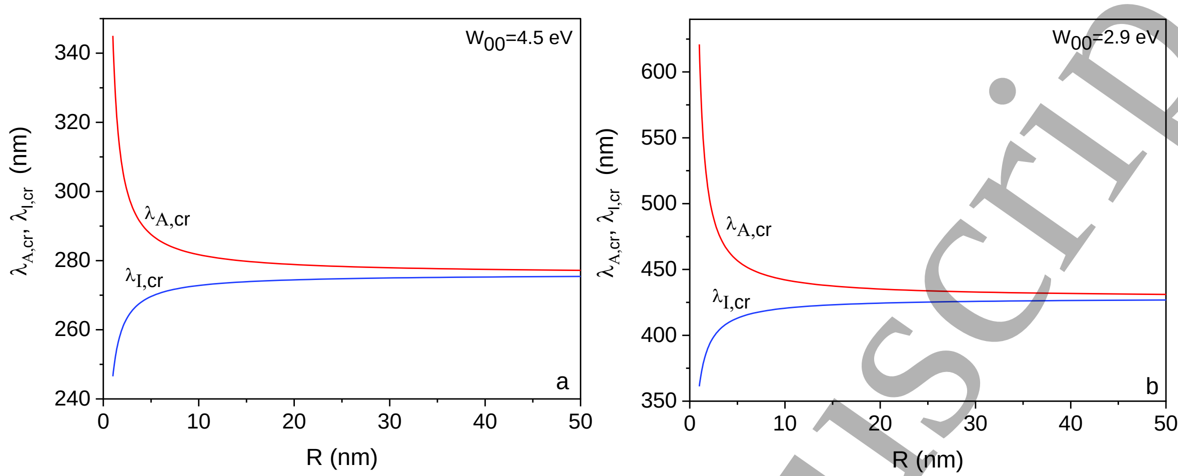

FIG. 4. Red borders for electron affinity and "ionization" for silver (a) and lithium (b) nanoparticles of different radii, without considering the Schottky effect

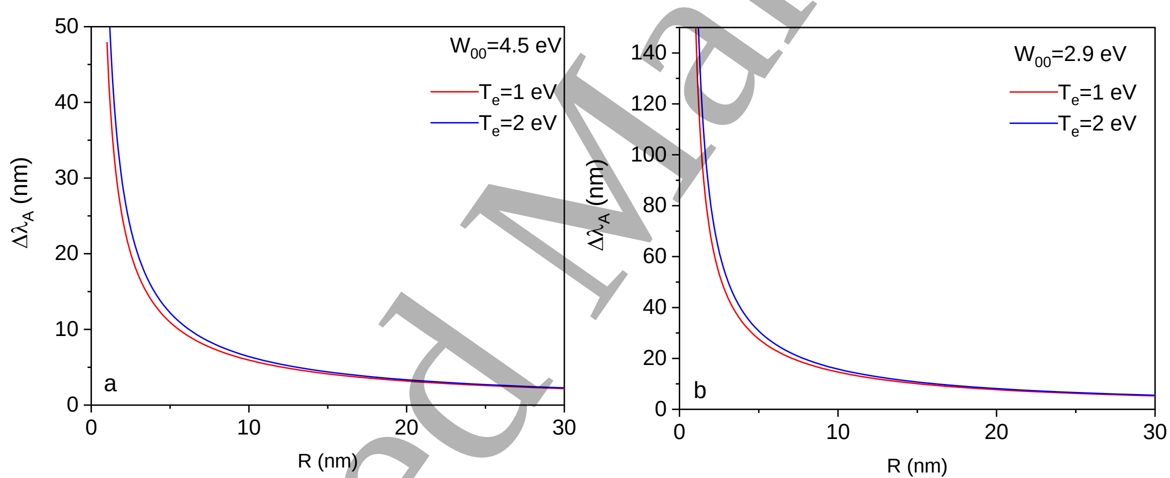

FIG. 5. Calculated changes in the red border of the laser radiation wavelength for the electron affinity, at which the photo-detachment of electrons from silver (a) and lithium (b) particles of different radii starts. A weakly ionized nitrogen plasma at T_i=300 K is considered.

Ideally, the applicability of the LSPD approach for particle size and charge measurements requires the absence of heating of particles by absorbed laser radiation, electron thermal emission, and the reverse charging of particles in the plasma. To fulfill the first two requirements, optimal characteristics of the laser pulse are required at which complete photo-detachment of electrons occurs while thermal emission is still negligible. It is possible that the cross section for photo-detachment of electrons depends not only on the size of the particle and its charge, but also on its temperature. At the same fluence and other parameters of the laser pulse, heating and radiation cooling do not depend on the radius, since the particle mass, absorption power of laser radiation and radiation losses all scale by r_p^3, [29], while heating and cooling in collisions with plasma and buffer gas particles $\propto r_p{}^2$ can be neglected during the pulse time.

Finally, we hope to experimentally validate the presented theory and explore its implications for charge and size measurements of dust particles in plasma using LSPD. The particle charge can be determined from a saturation of LSPD-induced changes of the electron density in the plasma (similar to Ref. [11]), while the size of particles can be deduced from the determination of the red border for the photo-effect. For nanoparticle generation, we propose to use a gas aggregation source (GAS) of metal nanoclusters utilizing ion-induced sputtering of a metal target substrate or electrode. Such GAS can be implemented as RF-biased discharge [30] or a magnetron-type plasma source [31] and [32]. These sources provide controllable generation of nanoparticles with relatively narrow size distributions. Depending on their operating conditions and the synthesis/growth time, the size of generated nanoparticles can be varied in the range of 1-100's nm. The generated nanoparticles can be injected into a characterization volume [34] which can be filled with a plasma generated by an external source. The size of the injected particles during the photo-detachment could be monitored by ex-situ analysis or by in-situ detection such as laser-induced incandescence diagnostics [33, 34] or four-wave mixing techniques [35].

Although the density of generated metal nanoparticles in GAS's is predicted to be rather small $\leq 10^8 - 10^9$ cm^{-3} (e.g. for copper nanoparticles of ≤ 1-6 nm [36, 37]), the detection of photodetached electrons with electrostatic Langmuir probes or microwave interferometry is feasible but can be challenging. For example, if copper clusters with a 6 nm diameter are injected by the gas aggregation source into a nitrogen plasma with parameters considered for Figs. 3-5, then from Eq. 2, these particles will be charged to about 5 and 10 electron charges for the floating potential of -2.65 and -4.75 V, respectively. Under such conditions, assuming a plasma electron density of 10^{10}- 10^{11} cm^{-3} (typical for glow discharges) and an injected dust particle density of ~ 10^8 cm^{-3}, a complete photo-detachment of electrons would result in changes of less than 10% of the electron density in the plasma. For these simplified considerations, the depletion of the plasma electron density by dust particles was not considered.

Note that in recent electron photo-detachment studies [11], LSPD from silicon and carbon-like nanoparticles of 100-300 nm resulted in an increase of the plasma electron density comparable to the magnitude considered in the above analysis. These changes were successfully measured using microwave cavity resonance spectroscopy [11]. For the validation of the theory of the red border changes presented in this paper, LSPD will need to be applied to much smaller metal nanoparticles of less than 10 nm (Fig. 4).

For implementation of the LSPD in the proposed experiments, a tunable pulsed laser system such as a PowerLite 8020 Nd:YAG laser which pumps a Horizon optical parametric oscillator (OPO) can be employed. With the output wavelength in the range of 192-2750 nm, laser pulse duration of ~10 ns, bandwidth of 3-10 cm^{-1} and pulse energy of 0.1-130 mJ, this tunable system can produce photons with energies of 0.5-6.4 eV. Such short pulse duration is sufficient to maintain the LSPD on a shorter timescale than a recharging of dust particles by plasma electrons. This energy range would cover the range of affinities and work functions for metal particles. A natural requirement for an accurate interpretation of the experimental data is that the width of the emission line of the tunable laser should be noticeably thinner than the changes in the critical wavelength shown in Fig. 5. Control over the laser pulse energy, photon energy and the beam size should allow us to obtain the necessary conditions for electron photo-detachment. By varying the energy or the laser spot size the laser intensity can be varied. For our example, for the above tunable laser system, the range of available laser intensity is $10^3\ \mathrm{W/cm^2} \leq I_L \leq 5\mathrm{x}10^{10}\ \mathrm{W/cm^2}$. Use of laser intensities higher than 10^7 W/cm^2 may be unwanted to prevent heating of particles to thermionic emission temperatures and to avoid effects of multi-photon induced photo-detachment [38, 39].

It is important to mention that there is obviously a limitation on the detection limit for the proposed LSPD. Among other factors mentioned above, this detection limit is determined by the resolution of the spectrometer used for measurements. Since modern spectrometers can reliably resolve in the angstrom range, a shift of the red border of 1 nm scale (e.g. Fig. 5) should be possible to resolve. Of course, variations of the electron temperature may additionally complicate measurements and obscure the actual shift. In this theoretical study, we assumed a steady state plasma. Our goal is to set a theoretical basis for experiments. Experiments are needed to validate these predictions and feasibility of such measurements.

In conclusion, the Schottky effect is predicted to decrease the energy of photons required for electron photo-detachment from metal particles negatively charged in plasma. It is shown that the critical wavelength of the laser at which the photo-detachment starts (the red border of the photoelectric effect) depends not only on the work function, but also on the charge of nanoparticles and their size. Our theory predicts that the smaller the size of the nanoparticles, the stronger the shift of the red border of the photo-detachment. This result is important for measurements of the charge and size of dust nanoparticles using a LSPD technique. Such measurements can provide valuable information required for modeling of plasmas for synthesis of nanomaterials and material processing applications. The particle charge can be determined from the measurement of a saturation of the electron density changes due to the photo-detachment using for example, microwave interferometry [11]. Then, the size of particles can be deduced from the measured red border for photoemission. The presented theory can also guide the selection of the LSPD laser wavelength and analysis of measured results.

Acknowledgement

We thank Dr. Yerbolat Ussenov and Mr. Brian Jensen of Princeton University for fruitful discussions.

This work was performed under the U.S. Department of Energy through contract DE-AC02-09CH11466.

References

1. V. E. Fortov, G. E. Morfill, "Complex and Dusty Plasmas" (CRC Press, Taylor & Francis Group, 2019)
2. P. K. Shukla and A. A. Mamun, "Introduction to Dusty Plasma Physics" (Bristol: Institute of Physics Publishing, 2002)
3. R. Merlino and J. Goree, Physics Today 57, 32 (2004)

4. E. Thomas Jr., R. L. Merlino and M Rosenberg, Plasma Phys. Control. Fusion 54, 124034 (2012)
5. J. Winter, Plasma Phys. Control. Fusion 46 B583 (2004).
6. A. Bouchoule (Ed.), "Dusty Plasmas: Physics, "Chemistry and Technological Impacts in Plasma Processing" (John Wiley, New York, 1999).
7. Y. Watanabe, Plasma Phys. Control. Fusion 39, A59 (1997)
8. U. R. Kortshagen, R. M. Sankaran, R. N. Pereira, S. L. Girshick, J. J. Wu, and E. S. Aydil, Chem. Rev. 116, 11061 (2016).
9. O. Volotskova, I. Levchenko, A. Shashurin, Y. Raitses, K. Ostrikov, M. Keidar, Nanoscale 2010, 2, 2281)
10. W. W. Stoffels, M. Sorokin, J. Remy, Faraday Discuss., 137, 115 (2008)
11. T. J. A. Staps, T. J. M. Donders, B. Platier and J. Beckers, J. Phys. D: Appl. Phys. 55, 08LT01 (2022)
12. C.A. Feigl, B. Motevalli, A.J. Parker, B. Sun, S. Barnard, Nanoscale Horiz., 4, 983 (2019)
13. M Bacal, Plasma Sources Sci. Technol. 2 190 (1993)
14. G. Al Makdessi, A. Hamdan, J. Margot and R. Clergereaux, Plasma Sources Sci. Technol. 26, 085001 (2017)
15. L. J. Overzet, J. H. Beherman and J. T. Verdeyen, J. Appl. Phys. 66 1622 (1989)
16. O. Havnes, M. Kassa, J. Geophys. Res., 114, D 09209 (2009)
17. R. L. Heinisch, F. X. Bronold, and H. Fehske, "Surface Electrons at Plasma Walls" in Complex Plasmas, Ed. By M. Bonitz et al., (Spirnger, Swicthzerland, 2014)
18. L.G. Christophorou, P. G. Datskos, H. Faidas, J. Chem. Phys., 101, 6728 (1994)
19. J.C. Weingartner, B.T. Draine, ApJS, 134, 263 (2001)
20. W. Schottky, Physik. Zeitschr. 15, 872 (1914)
21. E. Stoffels, W. W. Stoffels, G. M. W. Kroesen and F. J. de Hoog, J. Vacuum Sci. Technol. A 14, 556 (1996)
22. J. Goree, Plasma Sources Sci.Technol. 3, 400 (1994)
23. R. V. Kennedy, J. E. Allen, J. Plasma 2003
24. L. D. Landau and E. M. Lifshitz, "Electrodynamics of Continuous Media", 2nd ed. (Pergamon Press, Oxford, 1984)
25. J.P. Perdew, Phys. Rev. B, 37, 6175 (1988)
26. M. P. J. van Staveren, H. B. Brom, L. J. de Jongh, Y. Ishii, Phys. Rev. B35, 7749 (1987)
27. J.M. Smith, AIAA J. 3, 648 (1965)
28. CRC Handbook of Chemistry and Physics version, Ed. W.M. Haynes, 97th Edition (CRC Press 2017)
29. H.A. Michelsen, et al., Appl. Phys. B 87, 503 (2007)
30. S.A. Orazbayev, A.U. Utegenov, A.T. Zhunisbekov, M. Slamyiya, M.K. Dosbolayev, T.S. Ramazanov, Contrib. Plasma Phys. 58, 961 (2018)
31. M. Ganeva, T. Peter, S. Bornholdt, H. Kersten, T. Strunskus, V. Zaporojtchenko, F. Faupel, and R. Hippler, Contrib. Plasma Phys. 52, 881 (2012)
32. T. Momin and A. Bhowmick, Rev. Sci. Instrum. 81, 075110 (2010)
33. S. Yatom, J. Bak, A. Khrabryi, and Y. Raitses, Carbon 117, 154 (2017)
34. F. M. J. H. van de Wetering, W. Oosterbeek, J. Beckers, S. Nijdam, E Kovačević and J Berndt, J. Phys. D: Appl. Phys. 49 295206 (2016)
35. A. Gerakis, Y.-W. Yeh, M. N. Shneider, J. M. Mitrani, B. C. Stratton, and Y. Raitses, Phys. Rev. Appl. 9, 014031 (2018)

36. T. Momin and A. Bhowmick, Rev. Sci. Instrum. 81, 075110 (2010)
37. K. Fujioka, PhD Thesis, Kinetic Monte Carlo Simulations of Cluster Growth in Magnetron Plasmas, the Christian-Albrecht University of Kiel, Kiel, Germany 2015
38. W. W. Smith, C. Y. Tang, C. R. Quick, H. C. Bryant, P. G. Harris, A. H. Mohagheghi, J. B. Donahue, R. A. Reeder, H. Sharifian, J. E. Stewart, H. Toutounchi, S. Cohen, T. C. Altman, D. C. Risolve, J. Opt. Soc. Am. B, 8, 17 (1991)
39. D.S. Bursh, S. J. Smith, L. M. Branscomb, Phys. Rev. 112, 171 (1958).